

Extended Utility of Molten-Salt Chemistry – Unprecedented Synthesis of a Water-Soluble Salt-Inclusion Solid Comprised of High Nuclearity Vanadium Oxide Clusters

Wendy L. Queen, J. Palmer West, Joan Hudson, and Shiou-Jyh Hwu*

Department of Chemistry, Clemson University, Clemson, SC 29634-0973

- Figure S1: Powder X-ray diffraction (PXRD) pattern (blue line) of the as-prepared sample from the stoichiometric synthesis of $\text{Cs}_{11}\text{Na}_3(\text{V}_{15}\text{O}_{36})\text{Cl}_6$. The calculated pattern based on the single crystal structure solution is included for comparison. A couple of impurity peaks with minor intensities are marked with asterisks.
- Figure S2: (top) The connectivity of the cation units within the *ab* plane occurs *via* Cs–Cl bonds (red solid lines). Only the polyhedral view of a single unit is shown for clarity. Also, the relative positions of the polyoxovanadate $[\text{V}_{15}\text{O}_{36}\text{Cl}]^{9-}$ cluster (POV15) and the two additional cesium cations, Cs(3,4), are included for reference. (bottom) For the convenience, the $[\text{Cs}_9\text{Na}_3\text{Cl}_5]$ ($\equiv \text{Cs}_{6 \times 1}\text{Cs}_{6 \times (1/2)}\text{Na}_{3 \times 1}\text{Cl}_{2 \times 1}\text{Cl}_{3 \times 1}$) cation unit in $\text{Cs}_{11}\text{Na}_3(\text{V}_{15}\text{O}_{36})\text{Cl}_6$ showing again the connectivity between two chlorine-centered, anti-trigonal prisms ($\text{Cl}@\text{Na}_3\text{Cs}_3$ in polyhedral drawing) and three Cl-octahedral ClNa_2Cs_4 (in ball-and-stick representation) units.
- Figure S3: Molar magnetic susceptibility, χ (\circ), and the inverse molar magnetic susceptibility, χ^{-1} (\bullet) collected on $\text{Cs}_{11}\text{Na}_3\text{V}_{15}\text{O}_{36}\text{Cl}_6$ with an applied field of 0.01T. The inset shows the magnetic moment, μ_{eff} , plotted as a function of temperature.

Figure S1: Powder X-ray diffraction (PXRD) pattern (blue line) of the as-prepared sample from the stoichiometric synthesis of $\text{Cs}_{11}\text{Na}_3(\text{V}_{15}\text{O}_{36})\text{Cl}_6$. The calculated pattern based on the single crystal structure solution is included for comparison. A couple of impurity peaks with minor intensities are marked with asterisks.

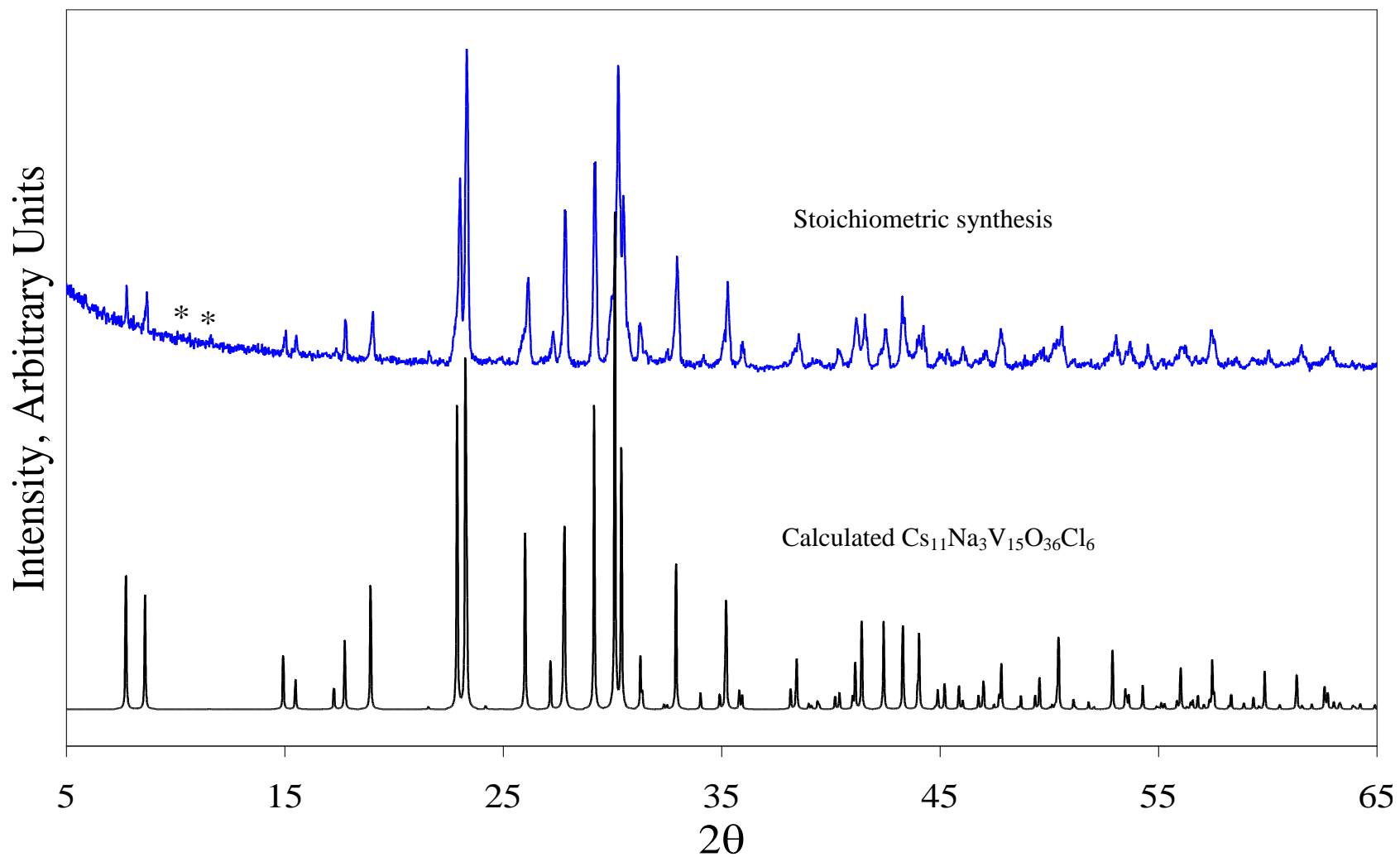
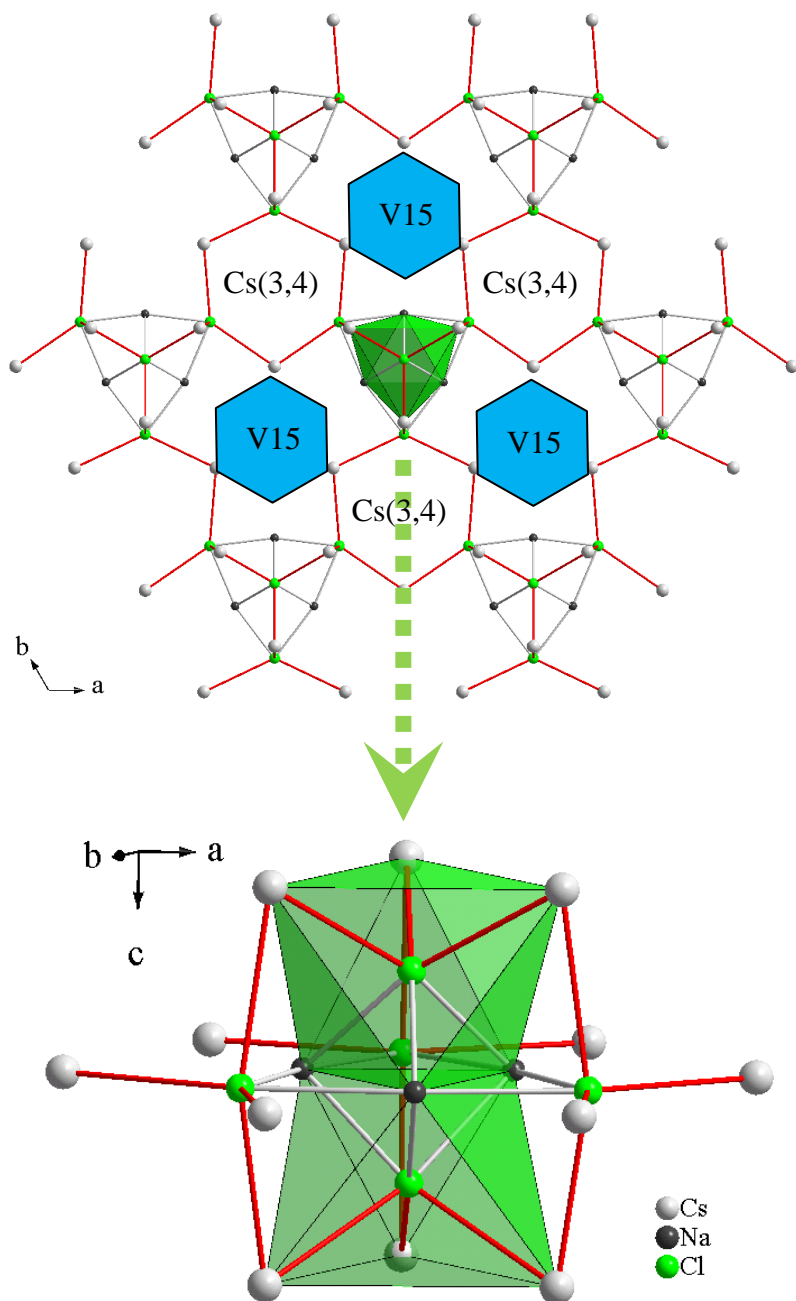


Figure S2: (top) The connectivity of the cation units within the *ab* plane occurs *via* Cs–Cl bonds (red solid lines). Only the polyhedral view of a single unit is shown for clarity. Also, the relative positions of the polyoxovanadate $[V_{15}O_{36}Cl]^{9-}$ cluster (V15) and the two additional cesium cations, Cs(3,4), are included for reference. (bottom) For the convenience, the $[Cs_9Na_3Cl_5]$ ($\equiv Cs_{6 \times 1}Cs_{8_{6 \times (\frac{1}{2})}}Na_{3 \times 1}Cl_{2 \times 1}Cl_{3 \times 1}$) cation unit in $Cs_{11}Na_3(V_{15}O_{36})Cl_6$ showing again the connectivity between two chlorine-centered, anti-trigonal prisms (Cl@Na₃CS₃ in polyhedral drawing) and three Cl-octahedral ClNa₂Cs₄ (in ball-and-stick representation) units.



Note: The Na–Cl bond distances are 2.752(7) Å and 3.039(7) Å; Cs–Cl are 3.293(3) Å, 3.486(1) Å, 3.549(1), and 3.620(3) Å, which are comparable with 2.83~2.99 Å and 3.48~3.59 Å, respectively, the sum of Shannon crystal radii.

Figure S3: Molar magnetic susceptibility, χ (\circ), and the inverse molar magnetic susceptibility, χ^{-1} (\bullet) collected on $\text{Cs}_{11}\text{Na}_3\text{V}_{15}\text{O}_{36}\text{Cl}_6$ with an applied field of 0.01T. The insets show the temperature dependence of (top left hand corner) the overlapped χT at two different fields, 100 Oe and 5000 Oe, and (lower right hand corner) the magnetic moment, μ_{eff} .

